



	Experiment title: Time-resolved <i>in-situ</i> GISAXS studies of the mesoscopic roughness during homoepitaxial electrodeposition on Au(001)	Experiment number: SI-2282
Beamline: ID32	Date of experiment: from: 20 June 2011 to: 28 June 2011	Date of report: 14 February 2012
Shifts: 18	Local contact(s): Dr. Parasmani Rajput	<i>Received at ESRF:</i>
Names and affiliations of applicants (* indicates experimentalists): M. Ruge ^{1*} , F. Golks ^{1*} , J. Stettner ^{1*} , P. Rajput ² , J. Zegenhagen ² , O.M. Magnussen ^{1*} ¹ Institute of Experimental and Applied Physics Christian-Albrechts-University Kiel Olshausenstr. 40 24098 Kiel, Germany ² European Synchrotron Radiation Facility		

Report:

The electrochemical deposition of metals is a subject of substantial basic research, motivated by current technologies as well as future applications. To obtain a better fundamental understanding of electrodeposition processes we studied metal electrode surfaces *in-situ* during deposition in aqueous electrolytes by grazing incidence small angle x-ray scattering (GISAXS), using the homoepitaxial growth on Au(001) electrodes as an example.

In the present work we performed the first GISAXS studies at the ID32 and even the first *in-situ* GISAXS measurements at the electrolyte/metal interface. Measurements were performed by using our established "hanging meniscus" transmission x-ray cell using a photon energy 22.5 keV. The scattered intensity was detected with a 2D pixel detector (Dectris Pilatus 300K-W), which was installed at a distance of 1.5 m behind the sample. To prevent detector saturation or damage due to the primary and specularly reflected beam, a beamstop consisting of a tantalum sheet (width 2 mm) was fixed directly in front of the detector.

In the previous beamtime SI-1194 we determined kinetic growth behaviour of homoepitaxial growth on Au(001) in 0.1 M HCl + HAuCl₄ 0.5 mM in dependence of the applied electrode potential and the electrodeposition rate [1]. Based on these results the evolution of the lateral surface structure during deposition for various potentials in the regime of multilayer growth from -0.10 to 0.15 V_{Ag/AgCl} in steps of 0.05 V was investigated in the current work. As in our previous growth mode studies, the surface was smoothed at 0.60 V_{Ag/AgCl}, i.e. in the regime of step flow growth, before the step to more negative potentials was performed. Frames were taken with a rate of 0.5 Hz.

At 0.60 V_{Ag/AgCl}, the two-dimensional intensity distribution on all detector frames was almost identical, showing scattering contributions from the static step arrangement resulting from the sample miscut (Fig. 1, 2a)). Fig. 1 shows the intensity distribution taken by a detector frame, with respect to the reciprocal space coordinates, illustrating the combined q_x , q_z -dependence in the vertical direction on the detector. To gain information about the lateral structures on the Au(001) surface, we transformed the detector frames into the reciprocal plane (q_x , q_y) parallel to the sample surface (Fig. 2). The intensity distribution at 0.60 V_{Ag/AgCl} (Fig. 2a)) exhibits two characteristic streaks, which are perpendicular to each other, originating from kinked step edges parallel to [100] and [010] [2]. In multilayer growth the pattern exhibits an additional circular ring (radius q_r) around the specularly reflected beam (Fig. 2b)).

To separate the static scattering contributions from the diffuse scattering that belongs to the growing structures on the terraces (e.g. islands), we averaged over the detector frames taken at 0.60 V_{Ag/AgCl} and subtracted this contribution from the frames taken in the potential regime of multilayer growth.

On the unreconstructed surface we found an isotropic surface morphology during multilayer growth (Fig. 3a)). Multilayer growth on (partially) reconstructed surfaces results in an anisotropic surface morphology where the intensity along the [110] and $[\bar{1}10]$ direction is significantly increased (Fig. 3b)). This behaviour resembles that found in recent STM results of Vaz-Dominguez and Cuesta for much lower growth rates and layer-by-layer growth, which show that island growth on the unreconstructed parts of the surface occur predominantly along the "hex" stripes, leading to strongly anisotropic surface structures [2]. At all potentials the preferential size $L=2\pi/q_r$ of lateral structures on the single crystal surface increases with applied potential and can be described by a well-defined power law (Fig. 4). Surprisingly, the exponent $\nu = 0.26 \pm 0.02$ is potential independent, i.e. independent of the potential dependent surface mobility as well as the crystalline structure of the electrode (reconstructed/unreconstructed surface).

Furthermore, the diffusely scattered intensity on the ring increases with time, indicating increasing surface roughness during multilayer growth. The quantitative data analysis should allow to study the scaling behaviour of the rms-roughness $\sigma(t)$ and is still in progress.

These first *in-situ* GISAXS studies demonstrate the great potential of this technique for determining the time-dependent surface morphology during electrochemical growth. Data of this type can currently not be obtained by any other method, making *in-situ* GISAXS an exciting novel tool for clarifying fundamental open questions concerning these technologically important processes.

References

- [1] K. Krug, J. Stettner, O.M. Magnussen: *Phys. Rev. Lett.* **96**, 246101 (2006).
- [2] C. Vaz-Dominguez, A. Cuesta: *Electrochim Acta* **56**, 6847 (2011).

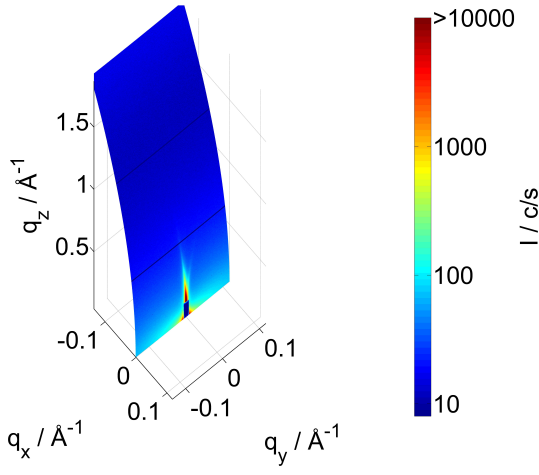


Figure 1: The detector frame at 0.60 $V_{Ag/AgCl}$ and $\alpha_i = 0.2^\circ$ in reciprocal space (q_x , q_y parallel to the sample surface).

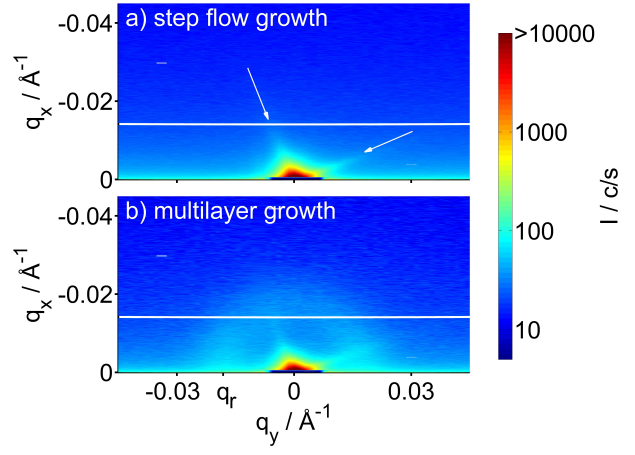


Figure 2: Intensity distribution with respect to q_x , q_y for **a)** step flow growth (0.60 $V_{Ag/AgCl}$). The streaks marked by arrows are perpendicular to each other (see text). The intensity distribution for **b)** multilayer growth (0.10 $V_{Ag/AgCl}$, deposition time $t=30$ s) shows an additional circular ring (radius q_r).

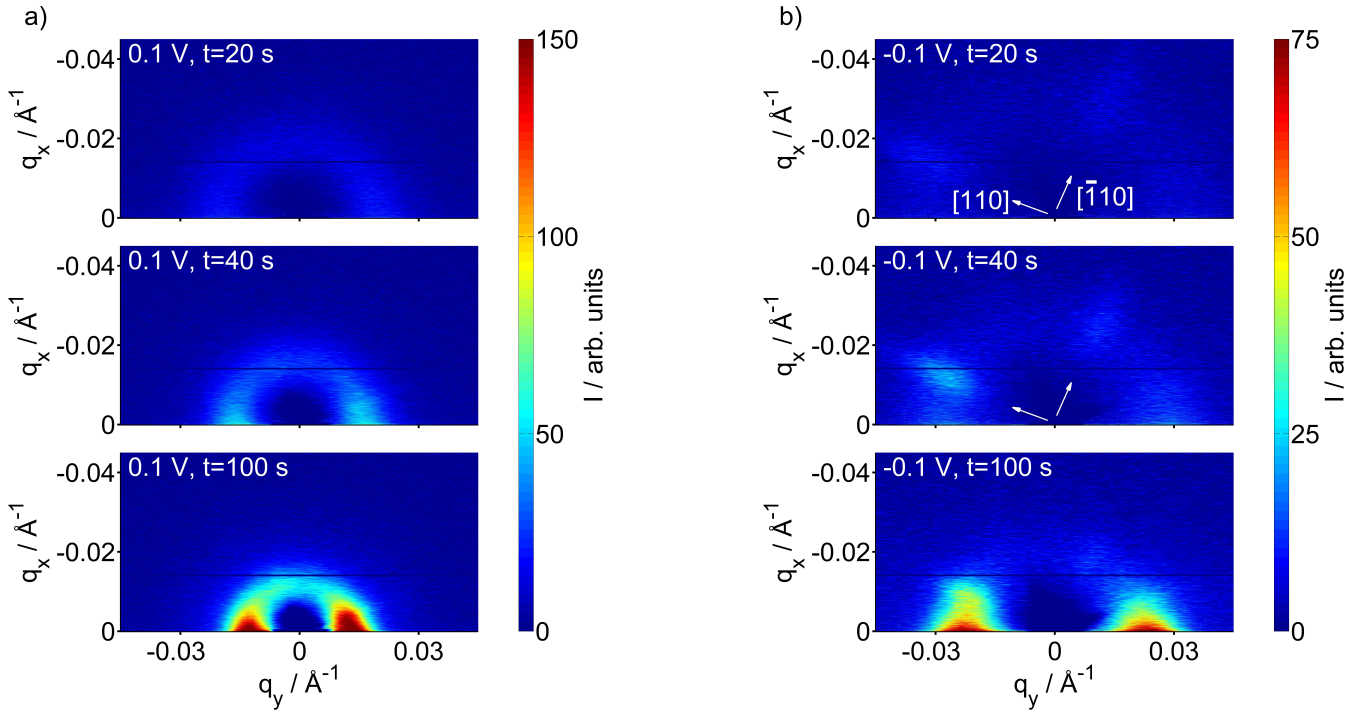


Figure 3: Distribution of separated intensity at different stages of multilayer growth on **a)** the unreconstructed (0.10 $V_{Ag/AgCl}$), and **b)** the hex-reconstructed (-0.10 $V_{Ag/AgCl}$) Au(001) surface.

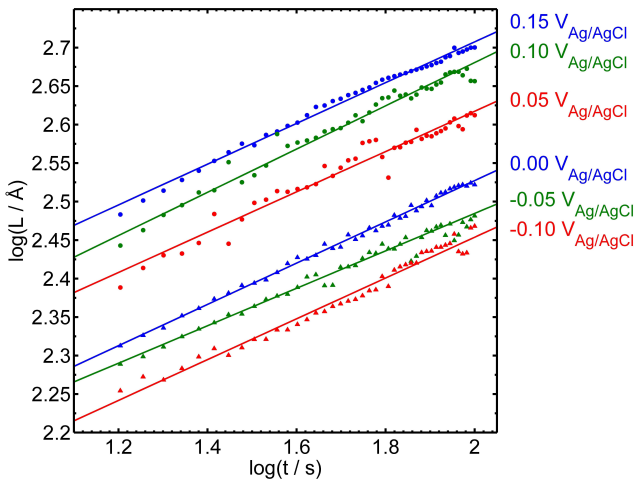


Figure 4: Preferential size $L=2\pi/q_r$ of lateral surface structures as a function of deposition time t for various deposition potentials.